

## PX ANDROMEDAE AND THE SW SEXTANTIS PHENOMENON

COEL HELLIER<sup>1</sup> AND E. L. ROBINSON

Department of Astronomy, University of Texas, Austin, TX 78712

Received 1994 May 3; accepted 1994 June 2

### ABSTRACT

We show that the emission-line peculiarities of PX And and other SW Sex stars can be explained by an accretion stream which overflows the initial impact with the accretion disk and continues to a later reimpact. The overflowing stream is seen projected against a brighter disk and produces the “phase 0.5 absorption” features. Emission from the reimpact site produces the high-velocity line wings which alternate from red to blue on the orbital cycle. We conclude that substantial disk overflow is the property distinguishing SW Sex stars from other cataclysmic variables.

*Subject headings:* accretion, accretion disks — novae, cataclysmic variables — stars: individual (PX Andromedae)

### 1. INTRODUCTION

A common assumption in cataclysmic variable research has been that the white dwarf is surrounded by an axisymmetric accretion disk. Departures from symmetry caused by the accretion stream from the secondary star are considered to be confined to the low-velocity outer regions of the disk and hence affect only the core of the observed emission lines. However, recent work has produced a growing list of discrepant objects with anomalous line wings that cannot be explained by a Keplerian disk.

A group of nova-like objects showing particularly striking line profiles—with high-velocity wings varying from the red to the blue side on the orbital cycle—were called SW Sex stars by Thorstensen et al. (1991). They are all eclipsing systems with orbital periods of 3–4 hr and may have relatively high mass transfer rates (Shafter 1992). The line profiles often show absorption in their cores near phase 0.5 (Szkody & Piche 1990; Thorstensen et al. 1991).

Several explanations have been proposed for such departures from the expected disk emission, including disruption of the disk by a magnetic field, emission from a disk wind, and Stark broadening (e.g., Williams 1989; Lin, Williams, & Stover 1989; Dhillon, Marsh, & Jones 1991). However, the only idea that directly addresses the requirement for an asymmetry locked to the orbital cycle is the proposal that the accretion stream is not stopped by its initial impact with the disk but continues flowing over the disk. This was shown to be plausible by the calculations of Lubow (1989) and has been suggested as an explanation for SW Sex stars by Shafter, Hessman, & Zhang (1988), Szkody & Piche (1990), and Thorstensen et al. (1991), while Hellier et al. (1989) adopted it for EX Hya during outburst. Further, this idea might also explain periodicities in the X-ray light curves of FO Aqr and GK Per (Hellier 1993; Hellier & Livio 1994). In this *Letter* we investigate the disk overflow model by calculating the line profiles expected and comparing them to new spectroscopy of the SW Sex star PX And (PG 0027 + 26). Other work on this star has been reported by Thorstensen et al. (1991) and Still, Dhillon, & Jones (1994).

### 2. THE EPHEMERIS

To secure the phasing of our spectroscopy we obtained an orbital cycle of photometry of PX And on each of the nights 1993 September 8 and November 6. The light curves (Fig. 1) show the prominent flickering and variable eclipse profiles typical of PX And. We measured the eclipse times by fitting with a Gaussian. The results are shown in Table 1 together with timings used by Thorstensen et al. (1991). They give an unambiguous cycle count with an RMS residual of only 90 s, comparable with the time resolution of the data. The best-fitting ephemeris is

$$\text{HJD}_{\text{eclipse}} = 2,449,238.8369(6) + 0.14635278(7)E.$$

### 3. SPECTROSCOPY

Between 1993 October 16 and 22 we observed PX And with the McDonald Observatory 2.1 m telescope and ES2 spectrograph, covering the H $\alpha$  line with 2 Å resolution. We obtained 250 spectra, each with a 5 minute integration time, covering seven orbital cycles. The sum of these spectra is shown in Figure 2. We have allocated the spectra to phase bins on the orbital cycle and display the result both in Figure 3 and as a false-color diagram in Figure 4 (Plate L13). Orbital phase 1 is eclipse, according to the above ephemeris. The enhanced intensity at this phase indicates that the line emission is eclipsed to a lesser degree than the continuum, since in constructing the figure, each spectrum was normalized to the continuum.

The line profile has stationary twin peaks near its center, characteristic of a high-inclination accretion disk. In addition we see the distinguishing feature of SW Sex stars, a high-velocity S-wave producing a prominent red wing at phase 1 and a corresponding blue wing at phase 0.5. We have computed the Doppler tomogram (see Marsh & Horne 1988) of this image using the Fourier-filtered back-projection technique (Fig. 5). The data from the two phase bins near eclipse were not included. The double-peaked profile produces the central ring in the tomogram. The line wings cause the enhanced emission to its left.

### 4. INTERPRETATION

The double-peaked component which produces the ring structure in the tomogram is probably disk emission. That the

<sup>1</sup> Hubble Fellow.

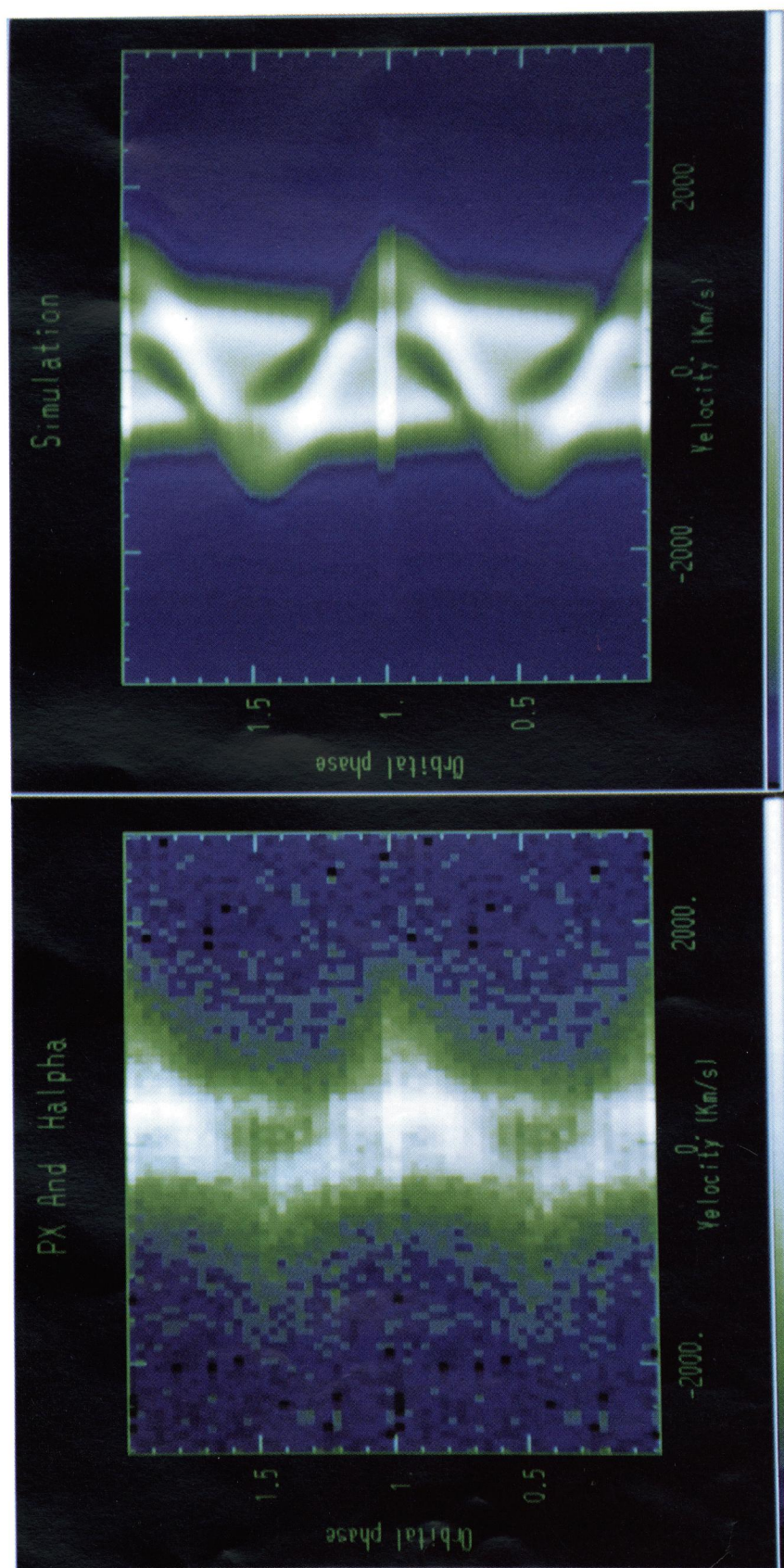


FIG. 4.—A false-color plot of the emission-line profiles of P X And as a function of phase. The left-hand panel shows our H $\alpha$  data from 1993 October; the right-hand panel shows the simulated profiles expected from an accretion stream overflowing the accretion disk. The simulation consists of the double-peaked profile of a Keplerian disk; a higher velocity S-wave from the stream region colored black in Fig. 6; an absorption S-wave in the line core, from the stream region colored white; and enhanced intensity at phase 1 to simulate the eclipse.

HELLIER & ROBINSON (see 431, L107)

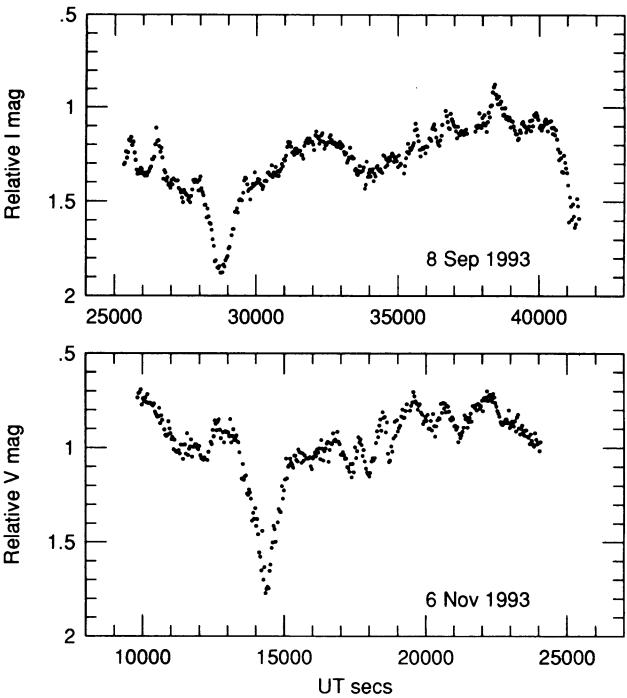


FIG. 1.—Photometry of PX And using the McDonald 0.8 m and a CCD camera with an *I* filter (September 8) and a *V* filter (November 6). Magnitudes are relative to the brighter star 2.5 SW.

double peaks are nearly stationary indicates a low orbital velocity of the white dwarf and hence a high mass ratio. The strongly asymmetric line wings preclude a reliable estimate of the orbital velocity; however, we can use circular symmetry to judge the centroid of the ring in the tomogram, giving  $K_1 \lesssim 80 \text{ km s}^{-1}$  and hence a mass function of  $\lesssim 0.0077 M_\odot$ . The radius of the ring is  $\sim 400 \text{ km s}^{-1}$ . Interpreting this as a Keplerian velocity implies an outer disk radius greater than the primary's Roche lobe, suggesting that the outer disk is sub-Keplerian by  $\sim 20\%$ .

In a dwarf nova such as U Gem, the S-wave is confined to the line core, roughly bounded by the double peaks of the disk

TABLE 1

ECLIPSE TIMES OF PX ANDROMEDAE

Cycle	HJD − 2,440,000
−9955 .....	7,781.895
−9949 .....	7,782.774
−9941 .....	7,783.943
−9921 .....	7,786.872
−9920 .....	7,787.017
−9914 .....	7,787.896
−9907 .....	7,788.920
−9901 .....	7,789.798
−9900 .....	7,789.944
−9894 .....	7,790.824
−9893 .....	7,790.969
−9887 .....	7,791.848
−9498 .....	7,848.776
−9492 .....	7,849.654
−9491 .....	7,849.803
−9472 .....	7,852.584
−2023 .....	8,942.764
0 .....	9,238.83776
402 .....	9,297.67098

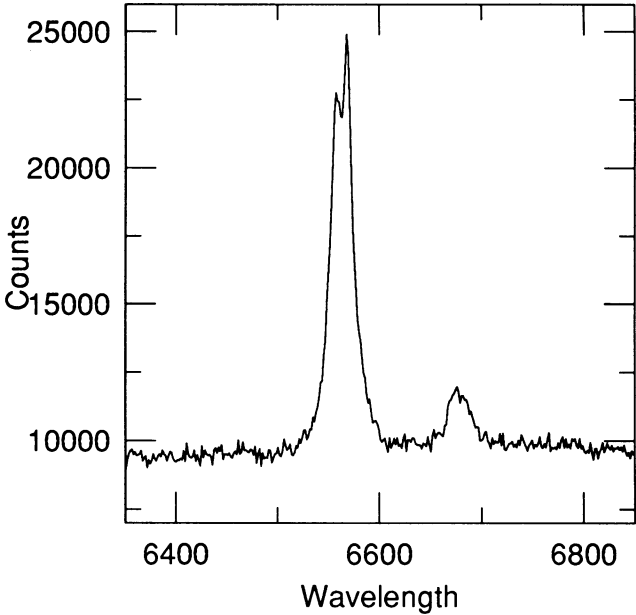


FIG. 2.—The summed spectrum of PX And showing H $\alpha$  and He I  $\lambda 6678$  emission.

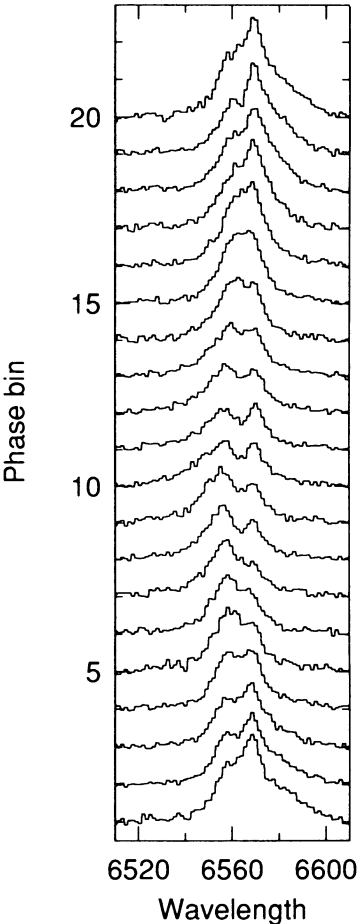


FIG. 3.—The line profile of H $\alpha$  in 20 phase bins around the orbital cycle, starting at eclipse.



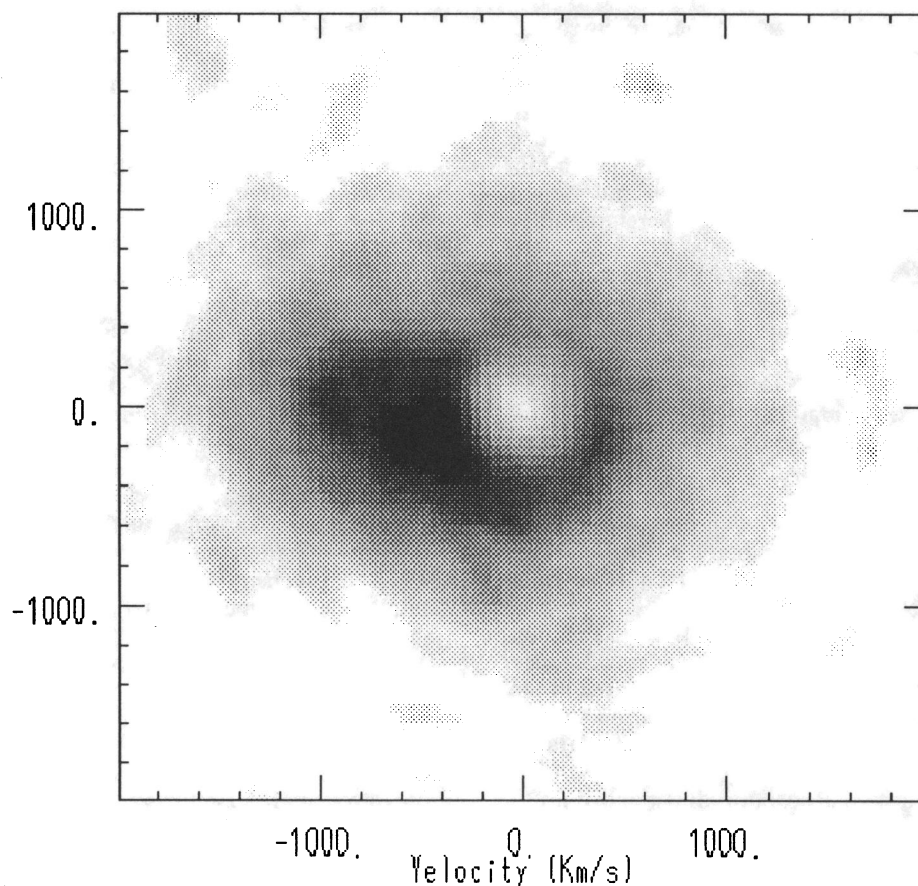


FIG. 5.—The Doppler tomogram of our H $\alpha$  spectra. We have not drawn on the white dwarf and secondary, since we have no reliable determination of their location. However, identifying the central ring with disk emission implies that the white dwarf is at its center. Since the phasing is secured by the eclipse, the secondary will be displaced upward by the orbital velocity. The accretion stream extends left toward the enhanced wing.

emission (e.g., Marsh et al. 1990). In PX And, however, the asymmetric emission has a much higher velocity and dominates the line wings. To investigate whether this can be explained by a stream overflowing the disk, we have written a program to simulate the line profiles expected from the accre-

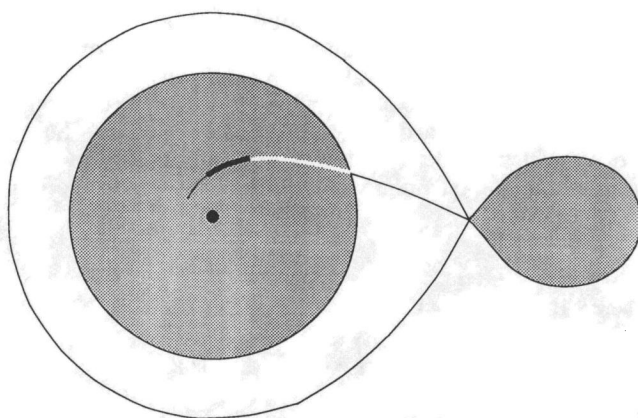


FIG. 6.—A schematic illustration of our disk overflow model. The stream trajectory is shown with a light line, continuing to the point where Lubow (1989) calculated it would reimpact the disk. The initial region of free-fall over the disk is shown in white and produces the absorption S-wave seen in the core of our simulation (Fig. 4). The heavy black line illustrates the region of re-impact, where enhanced emission produces the high-velocity S-wave. Our re-impact therefore occurs before that calculated by Lubow.

tion stream. We take the stream trajectory computed by Lubow & Shu (1975) and follow it to the point where Lubow (1989) calculated it would reimpact the disk close to the white dwarf (this is illustrated in Fig. 6). At each point along the stream we have calculated both the free-fall stream velocity and the Keplerian velocity of the disk segment underneath the stream. We accumulated the simulated profiles by adding Gaussians at these velocities, using a width of  $\sigma = 25\%$  of the local velocity. We calculated the projected profiles at each binary phase to create a phase-resolved image to compare with the data. To this we added the double-peaked profile of a Keplerian disk. In the simulation we have assumed a primary mass of  $1 M_{\odot}$ , a secondary mass of  $0.25 M_{\odot}$ , an inclination of  $75^{\circ}$ , and a disk radius of  $4 \times 10^{10}$  cm, but our results are not sensitive to reasonable variations in these parameters.

Figure 4 shows such a simulation. To reproduce the high-velocity S-wave, we add emission from the region of stream shown in black in Figure 6. For this section we have taken the velocity to be the mean of the stream and local disk velocities—supposing a strong interaction between the disk and stream. We have stopped this region short of the point where Lubow (1989) calculated the stream would re-impact. Emission from here would extend the line wing 0.2 in phase earlier, producing a red wing at phase 0.8 and a blue wing at phase 0.3 which are not seen in the data. Adding emission from farther upstream, nearer the edge of the disk, would produce an S-wave with a lower velocity and a later phasing—in other

words, the usual dwarf nova S-wave with a maximum redshift near phase 0.2. This, though, is also not seen in the data; indeed, the red wing of the double peak appears brighter *before* eclipse. We have therefore added *absorption* from the stream in the region from the edge of the disk onward (shown in white in Fig. 6) producing the absorption S-wave seen in the simulation. We suppose that the stream here is in free fall and viewed projected against the brighter disk; we have therefore added the absorption with the stream velocity only. The effect is to reduce the red peak after eclipse, reproducing the apparent enhancement before eclipse, when the disk profile and high velocity S-wave superpose (the same effect is seen in the tomogram).

The absorption S-wave also explains the “phase 0.5” absorption. For clarity we have made the simulated absorption slightly deeper than is justified by the H $\alpha$  data—it can be seen traveling from the red wing at phase 0.2 to the blue wing at phase 0.7 and back again. In lines such as  $\lambda$ 5175 (seen by Thorstensen et al. but not covered in our spectra), the absorption dominates. It has a lower velocity than the emission wing but has a similar velocity trend (see Fig. 10 of Thorstensen et al. 1991). This is reproduced by our simulation.

Near eclipse, we have artificially enhanced the line emission in our simulation to reproduce the larger equivalent width seen in the data. However, we have not simulated the eclipse of the disk or stream since parameters such as the inclination and the height of material above the disk are critical, and our data do not have sufficient time resolution to constrain them.

We can use the fact that the absorption dips remove up to  $\sim 10\%$  of the continuum flux in SW Sex stars to estimate the width of the accretion stream. The material in the stream is sufficient to be opaque in the lines (e.g., Hellier, Mason, & Cropper 1990), so the absorption depth requires that the stream cover  $\sim 10\%$  of the continuum source. If the light is dominated by a disk of radius  $r$ , we thus need a stream of width  $\sim \frac{1}{3}r$ . This is likely to be an overestimate since, in these high-inclination systems, disk flaring will reduce the contribution from the front of the disk relative to the rear, where the stream is located during phases of deep absorption. The opposite effect might explain why corresponding absorption effects are not generally seen at phases before eclipse (0.7–0.9)—as would be expected from our simulation. Here the stream would obscure the less visible near side of the disk and so would remove a smaller fraction of the total light.

## 5. DISCUSSION

We have shown that the major peculiarities of the emission line profiles of PX And can be explained as follows: The accretion stream overflows the accretion disk at its outer edge and continues on a quasi-ballistic trajectory. It is viewed projected

against a brighter disk and so produces the absorption features characteristic of SW Sex stars. The stream then reimpacts the disk closer in, producing enhanced line emission which explains the highly distorted line wings. The interaction of the stream and disk emission produces a line profile that is single peaked at some phases. In a star where the disk emission is a minor contribution, a single-peaked profile would always be seen, possibly explaining the single-peaked profiles, particularly of He II  $\lambda$ 4686, often seen in SW Sex stars (e.g., Dhillon et al. 1991). Alternatively, such profiles might require an additional emission component from a disk wind (e.g., Hoare 1994).

An absorption S-wave has also been seen in the intermediate polar FO Aqr (Hellier et al. 1990). This is reassuring since FO Aqr also shows evidence for disk overflow from the X-ray light curves (Hellier 1993). The difference is that in this magnetic system, the overflowing stream collides with the magnetosphere rather than the inner disk. EC 1931–59 shows a similar absorption component (Buckley et al. 1992), although here its phasing suggests an origin in the disk. Such features deserve further investigation—it may prove possible to explain effects such as the intensity variation of U Gem’s S-wave round the orbital cycle through the interaction of emission and absorption components.

In the light of our modeling we can ask the question: What is an SW Sex star? Thorstensen et al. (1991) introduced the term for stars which showed the peculiar line profiles and which were also eclipsing nova-like objects with orbital periods in the range 3–4 hr. We propose that the SW Sex stars are those in which an accretion stream overflowing the disk, rather than the disk itself, dominates the observed characteristics. There seems no reason to include only eclipsing systems—it is simply easier to observe the effects in a highly inclined binary—thus WX Ari (Beuermann et al. 1992; Hellier, Ringwald, & Robinson 1994) would qualify. We could also extend the term beyond nova-like objects with orbital periods of 3–4 hr: such systems might simply be more likely to have overflowing streams because of their higher accretion rates. However, if it turns out that disk overflow is a common property of cataclysmic variables, differing only in degree, a separate classification for these stars would become less useful.

We thank Tod Ramseyer for observing an eclipse of PX And, and we also thank John Thorstensen for forwarding eclipse timings and for valuable discussions on this star. Support for this work was provided by NASA through grant HF-1034.01-92A awarded by the Space Telescope Science Institute which is operated by the Association of Universities for Research in Astronomy, Inc., for NASA under contract NAS 5-26555.

## REFERENCES

- Beuermann, K., Thorstensen, J. R., Schwöpe, A. D., Ringwald, F. A., & Sahin, H. 1992, *A&A*, 256, 442  
 Buckley, D. A. H., O’Donoghue, D., Kilkenny, D., Stobie, R. S., & Remillard, R. A. 1992, *MNRAS*, 258, 285  
 Dhillon, V. S., Marsh, T. R., & Jones, D. H. P. 1991, *MNRAS*, 252, 342  
 Hellier, C. 1993, *MNRAS*, 265, L35  
 Hellier, C., & Livio, M. 1994, *ApJ*, 424, L57  
 Hellier, C., Mason, K. O., & Cropper, M. S. 1990, *MNRAS*, 242, 250  
 Hellier, C., Mason, K. O., Smale, A. P., Corbet, R. H. D., O’Donoghue, D., Barrett, P. E., & Warner, B. 1989, *MNRAS*, 238, 1107  
 Hellier, C., Ringwald, F. A., & Robinson, E. L. 1994, *A&A*, in press  
 Hoare, M. G. 1994, *MNRAS*, 267, 153  
 Lin, D. N. C., Williams, R. E., & Stover, R. J. 1988, *ApJ*, 327, 234  
 Lubow, S. H. 1989, *ApJ*, 340, 1064  
 Lubow, S. H., & Shu, F. H. 1975, *ApJ*, 198, 383  
 Marsh, T. R., & Horne, K. 1988, *MNRAS*, 235, 269  
 Marsh, T. R., Horne, K., Schlegel, E. M., Honeycutt, R. K., & Kaitchuck, R. H. 1990, *ApJ*, 364, 637  
 Shafter, A. W. 1992, *ApJ*, 394, 268  
 Shafter, A. W., Hessman, F. V., & Zhang, E. H. 1988, *ApJ*, 327, 248  
 Still, M. D., Dhillon, V. S., & Jones, D. H. P. 1994, *MNRAS*, in press  
 Szkody, P., & Piche, F. 1990, *ApJ*, 361, 235  
 Thorstensen, J. R., Ringwald, F. A., Wade, R. A., Schmidt, G. D., & Norsworthy, J. E. 1991, *AJ*, 102, 272  
 Williams, R. E. 1989, *AJ*, 97, 1752